Journal of Sound and Vibration (2001) **248**(3), 441–459
doi:10.1006/jsvi.2001.3797, available online at http://www.idealibrary.com on IDEAL®

ON THE CHARACTERISTIC POWER OF STRUCTURE-BORNE SOUND SOURCES

A. T. MOORHOUSE

Acoustics Research Unit, School of Architecture and Building Engineering, University of Liverpool, Liverpool L69 3BX, England. E-mail: a.t.moorhouse@liv.ac.uk

(*Received* 7 *January* 2000, *and in final form* 5 *March* 2001)

The paper deals with methods of independently characterizing sources of structure-borne sound. The concept of mirror power is introduced, which is the power delivered by a vibration source when connected to a passive receiver structure that is a mirror image of itself. A second quantity, the characteristic power is defined to be the dot product of the blocked force and free velocity vectors and this is shown to be four times the mirror power. In addition, expressions are given for the maximum available power from a source. These three concepts each provide, in a single value, an independent characterization of a structure-borne sound source. They are valid for multiple point and component contact as well as for contact over extended areas. The characteristic power (CP) is shown to be the most practical of the three, and examples of the CP of several real machine sources are given. It is shown that the emission from a source when installed is usually a fraction of the CP. This factor depends on the ratio of the source and receiver mobilities, and the trends in its behaviour can be predicted simply from the ratio of typical point mobilities of the source and receiver. CP thus provides an equivalent single point formulation for characterizing structure-borne sound sources.

1. INTRODUCTION

The objective of this paper is to present the concept of characteristic power (CP) as a possible characterization for structure-borne sound sources. Initially, the question is considered as to what is required from a source characterization. Designers, vendors and purchasers of machinery need reliable information about the "noisiness" of machines so that they can

(1) compare one source with another;
(2) compare sources with set limits;
(3) predict sound levels when installed;
(4) quantify the improvement of new low noise designs.

Sound power (L_w) meets all of these objectives for most airborne sound sources and is widely used and standardized. In the case of structure-borne sound sources, a characterization equivalent to L_w does not exist, partly because the power delivered varies from one installation to the next, being dependent not only on the source, but also on the structure to which the source is connected (the receiver).

To achieve aims (1) and (2) the source characterization must be presented as a single value. This does not rule out more detailed information, for example about the directivity, but it must be possible to express the essential source strength as a single (frequency dependent) quantity. In the case of airborne sources, this is usually achieved by the sound

0022-460X/01/480441 + 19 $35.00/0

power, expressed as a spectrum or with an appropriate frequency weighting. Comparisons can then be made on an overall basis or frequency by frequency. In the structure-borne case, it is usually the subsequent radiated sound that is of ultimate importance. It could then be argued that the only correct comparisons between sources are between the power radiated from connected structures when installed. Nevertheless, there may be also situations when it is desirable to compare sources directly, for example for development engineers comparing the source strength of their products before and after modification.

Regarding objective (3), the supplier of a vibrating component will not generally know how it is to be installed. For example, the same electric motor may end up bolted to a washing machine frame or connected rigidly to a concrete slab in a plant room. The structure-borne emission depends on the receiver structure, and hence is not a universally applicable source descriptor. To allow prediction of installed sound levels, the source characterization must be a property of the source, *independent* of the receiver.

If the source characterization one is seeking is to achieve objectives (1)–(4) above it must

(1) characterize the source's ability to deliver structure-borne sound power;
(2) be an independent property of the source;
(3) be able to be expressed as a single value;
(4) form a basis for the calculation of power delivered when installed.

A number of possible characterizations were suggested by Ten Wolde and Gadefelt in 1987 [1]. Since then, a significant development has been the introduction of a standard for measurement of the velocity of resiliently mounted machines [2], which in practice can be taken as equal to their free velocity. Free velocity is independent, and characteristic of the source activity. However, it cannot be collapsed to a single value if both translational and rotational velocities are present, because of their dimensional incompatibility. More significantly, whilst free velocity data is in a form which allows the excitation of connected structures to be calculated, it is insufficient by itself for such calculations, and must be accompanied by mechanical mobilities of both source and receiver structures. Blocked forces have the same problems as free velocities, but in any case are rarely dealt with because of practical difficulties of measurement.

Methods where the source is attached to a standardized receiver structure also have been tried, in particular the reception plate method [3]. However, although yielding a single value, the characterization is not independent, and does not usually allow the subsequent calculation of transmitted sound when installed. An exception could be the case of pumps which are always attached to pipes of the same diameter, and where an infinite pipe can be used as a standard receiver system without compromising independence of the source characterization [4]. Other methods which introduce simplifying assumptions, e.g., as in reference [5], are seldom applicable except within a narrow range of specific cases.

Verheij's equivalent forces have been used successfully for rank ordering of transmission paths [6]. However, they are in general dependent on the receiver structure, and therefore not truly independent. Ohlrich's energy methods, see for example reference [7], characterize the energetics of a machine, but assumptions are required to calculate the power in connected structures. Pinnington and Pearce [8] give a useful simplification by expanding the forces and velocities into a number of multipoles. This is applied to measurement of the power transmitted to a receiver structure, but they do not address the problem of independent source characterization.

The most promising approach is Mondot and Petersson's Source descriptor [9], which meets all criteria except independence for the case of multiple-point connected structures. An extension of their concept, which will be termed the characteristic power (CP) [10] shows promise of overcoming this problem and is investigated here.

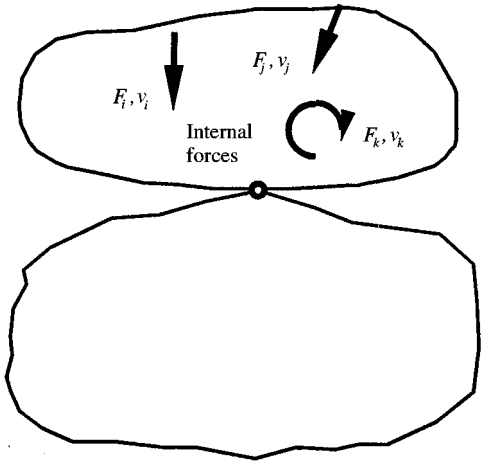

Figure 1. Source attached via a single point to a receiver.

2. CHARACTERISTIC POWER—THEORETICAL BACKGROUND

2.1. SINGLE POINT CASE

Initially, it is assumed that the source is linear, and that its vibration results from the action of internal forces f_O assumed independent of the attachment to any receiver (Figure 1). It is not known to what extent these assumptions are met in actual sources such as machines. Nevertheless, this black-box approach is a realistic starting point and is accepted in most previous studies. The activity of the source is then assumed to be uniquely characterized by its free velocity v_{sf} and its passive dynamic properties by the mobility at the contact point Y_S.

The complex power passing through the interface to a receiver structure is given by

$$\bar{Q} = |\bar{v}_{sf}|^2 \cdot \bar{Y}_R / |\bar{Y}_R + \bar{Y}_S|^2 \tag{1}$$

where $\bar{v}_{sf}$ is the r.m.s. free velocity $\bar{Y}_R$ and $\bar{Y}_S$ are the receiver and source mobility respectively. Throughout this paper, complex quantities are distinguished from real quantities by a bar. Equation (1) can be written in a dimensionless form, in terms of the complex ratio of receiver to source mobility $\bar{\alpha} = \bar{Y}_R/\bar{Y}_S$,

$$\bar{C}_c = \bar{Q}/|\bar{S}_c| = |\bar{\alpha}|/|1 + \bar{\alpha}|^2 \, e^{j\theta_R}, \tag{2}$$

where $\bar{S}_c = |\bar{v}_{sf}|^2/\bar{Y}_S^*$, and the "coupling factor" $\bar{C}_c$ has been introduced which will be discussed in more detail in section 4. θ_R is the phase of the receiver mobility.

The dimensionless power (magnitude and real part) from a source of a given phase when connected to a receiver of opposite phase is shown in Figure 2 (see also reference [9]). The power varies with $\bar{\alpha}$ in the same way as for electrical sources when delivering power into an impedance load. For high mobility sources ($|\bar{\alpha}| \ll 1$), the blocked condition is approximated and the power transfer is inefficient. At the other extreme, the free source condition is approached ($|\bar{\alpha}| \gg 1$) and the transfer of power is similarly inefficient. For any phase angle, a maximum occurs when $|\bar{\alpha}| = 1$.

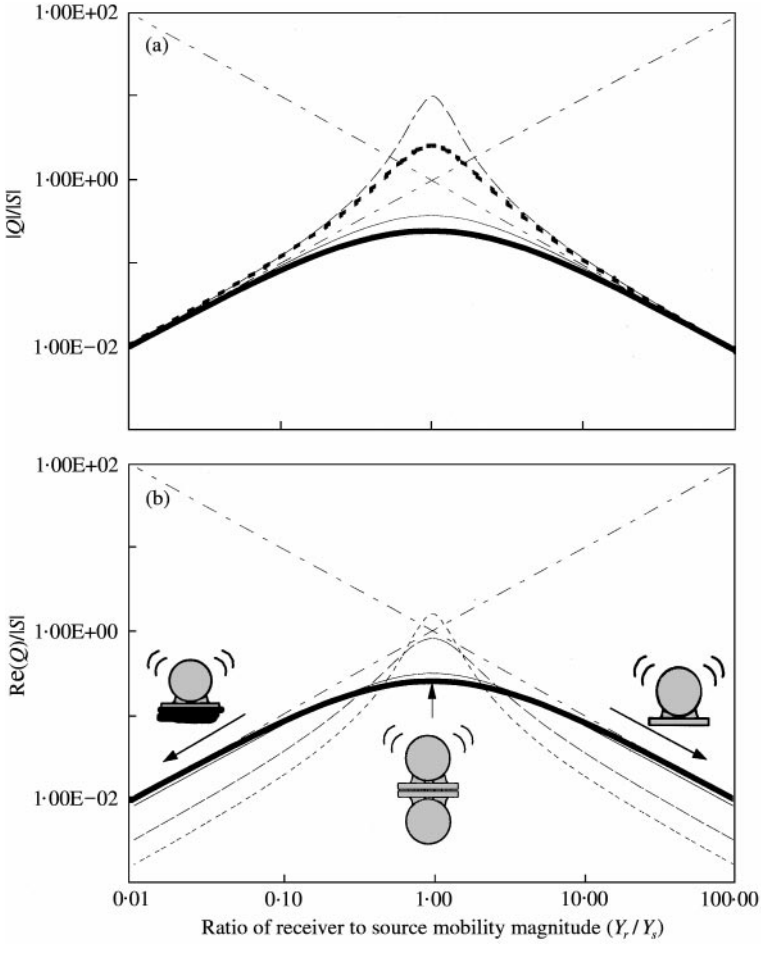

Figure 2. (a) Magnitude, and (b) real part of the power via a single contact point from a source of various mobility phases to a receiver of opposite phase. Diagonal lines indicate blocked and free source asymptotes. Phase $|\theta|$: ▬, 0; ——, $0{\cdot}2\pi$; – – –, $0{\cdot}4\pi$; – – – –, $0{\cdot}45\pi$.

The maximum power from a given source occurs when the mobilities of source and receiver are complex conjugate [9], and by substituting $Y_R = Y_S^*$ into equation (1); this is shown to be

$$\bar{Q}(\bar{Y}_R = \bar{Y}_S^*) = \bar{S}_a = |\bar{v}_{sf}|^2 \cdot \bar{Y}_S^* / [2\mathrm{Re}(\bar{Y}_S)]^2. \tag{3}$$

The real part is of particular interest and is given by the simpler expression

$$\mathrm{Re}[\bar{Q}(\bar{Y}_R = \bar{Y}_S^*)] = \mathrm{Re}(\bar{S}_a) = |\bar{v}_{sf}|^2 / 4\mathrm{Re}(\bar{Y}_S). \tag{4}$$

This is the maximum power that can be delivered by this source through its contact point to any receiver structure, and can realistically be termed the "maximum available power" (MAP). Figure 2(b) shows the real part of equation (2) for $\theta_R = -\theta_S$, that is the MAP, for four different values of source mobility phase.

Another point of interest in Figure 2 is when source and receiver mobility are equal (in magnitude and phase). By substituting $Y_R = Y_S$ into equation (1), the power is then seen

to be

$$\bar{Q}(\bar{Y}_R = \bar{Y}_S) = \bar{S}_m = |\bar{v}_{sf}|^2 \cdot 1/(4\bar{Y}_S^*), \tag{5}$$

which will be termed the "mirror" power, because it is the power delivered when the source is attached to a receiver which is a mirror image of itself. The magnitude of the mirror power is independent of source mobility phase (unlike MAP). For most sources, the magnitude of the mirror power is less than that of the MAP, but for the special case of a source of zero mobility phase the two are equal.

A further point of interest in Figure 2 is the intersection of the low mobility and high mobility source asymptotes. The power at this point is that obtained when the force is equal to the blocked force ($f_{bl} = v_{sf}/Y_s$), and the velocity to the free velocity, and is given by

$$\bar{Q}(f = f_{bl}, v = v_{sf}) = \bar{S}_c = |\bar{v}_{sf}|^2 \cdot (1/\bar{Y}_S^*). \tag{6}$$

This is 4 times the mirror power from equation (5). Mondot and Petersson call this value the source descriptor; here, it will be called the "characteristic power" (CP) (a new term is required as the generalization to multiple point contact to be given in the next section differs from that of Mondot and Petersson).

To summarize, three possible source characterizations have been developed in this section, namely, the mirror power, the characteristic power (CP) and the maximum available power (MAP). These ideas will now be extended to handle more realistic multiple point and component contact.

2.2. CHARACTERISTIC POWER FOR MULTIPLE POINT AND COMPONENT CASE

Consider now the case of contact at multiple discreet points, and with multiple component excitation (mixed rotational and translational degrees of freedom) as illustrated in Figure 3. Mondot and Petersson extended their source descriptor to deal with this case by introducing the concept of "effective mobility" [11]. However, the resulting multi-point source descriptor is a function of force distribution and thus of the receiver mobility and so does not fulfil the criterion of independence. Thus, the search will now be extended.

To find an expression for the "mirror power", the power delivered to an arbitrary receiver of mobility matrix, $\bar{\mathbf{Y}}_R$ is first considered, which, for contact at discreet multiple points is given by

$$\bar{Q} = \bar{\mathbf{v}}_{sf}^{\mathrm{H}}(\bar{\mathbf{Y}}_S + \bar{\mathbf{Y}}_R)^{-\mathrm{H}} \cdot \bar{\mathbf{Y}}_R \cdot (\bar{\mathbf{Y}}_S + \bar{\mathbf{Y}}_R)^{-1}\bar{\mathbf{v}}_{sf}, \tag{7}$$

where $\bar{Q}$ is the complex power through the interface, $\bar{\mathbf{Y}}_S$, $\bar{\mathbf{Y}}_R$ are the complex mobility matrices of the source and receiver, respectively, and $\bar{\mathbf{v}}_{sf}$ is the r.m.s. free velocity vector. H indicates the Hermetian transpose, i.e., $(\,)^{\mathrm{H}} = (\,)^{\mathrm{T}}$, and $(\,)^{-\mathrm{H}} = ((\,)^{\mathrm{T}})^{-1}$. Equation (7) is simply a development of equation (1) to multiple points and components. If the receiver is a mirror structure, then its mobility is identically equal to that of the source, so one can replace $\bar{\mathbf{Y}}_R$ by $\bar{\mathbf{Y}}_S$ to obtain

$$\bar{S}_m = \tfrac{1}{4}\bar{\mathbf{v}}_{sf}^{\mathrm{H}}(\bar{\mathbf{Y}}_S)^{-\mathrm{H}}\bar{\mathbf{v}}_{sf}. \tag{8}$$

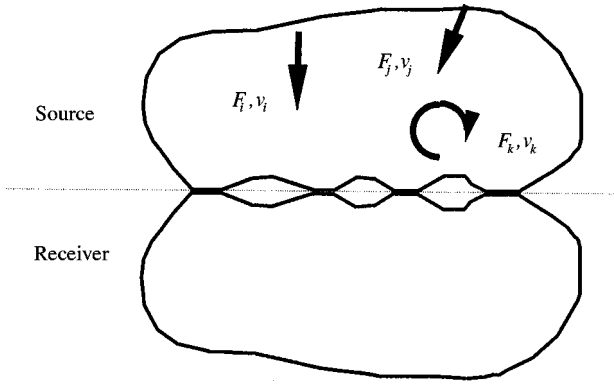

Figure 3. Source attached to mirror receiver.

By analogy with the single point case, the CP can be defined as 4 times the power into the mirror

$$\bar{S}_c = 4\bar{S}_m = \bar{\mathbf{v}}_{sf}^{\mathrm{H}}(\bar{\mathbf{Y}}_S)^{-\mathrm{H}}\bar{\mathbf{v}}_{sf}. \tag{9}$$

This is also equal to the dot product of the blocked force and free velocity vectors, which can be seen by substituting the blocked force vector, given by

$$\bar{\mathbf{f}}_{bl} = (\bar{\mathbf{Y}}_S)^{-1}\bar{\mathbf{v}}_{sf} \tag{10}$$

into equation (9), to give

$$\bar{S}_c = \bar{\mathbf{f}}_{bl}^{\mathrm{H}} \cdot \bar{\mathbf{v}}_{sf}. \tag{11}$$

Again, this is an extension of the single point case.

One notices that $\bar{S}_c$ collapses to Mondot and Petersson's source descriptor for single point contact and concludes that it is a generalization of their concept to multiple point and component excitation. The CP, as defined above, is characteristic of the source's ability to deliver power, is an independent property of the source and is a single, frequency-dependent value. Thus, it fulfils all the criteria set out in the introduction. Furthermore, there is no theoretical reason why this approach, being based on the concept of a mirror receiver, should not be valid for contact over extended surfaces as well as at discreet points.

The real part of the CP is 4 times the power permanently lost to the source by dissipation in the mirror. This is always positive or zero since there can be no net energy supplied by the passive receiver. The imaginary part of the CP is 4 times the power circulating through the interface. It can be positive or negative depending on whether the temporary storage of energy in the receiver during the vibration cycle is predominantly in the form of strain energy or kinetic energy.

Equation (11) implies another physical interpretation, i.e., that the CP is the power required to achieve the free velocity on an inoperative source through the application of external forces at the contact points. In such a situation, the applied forces would automatically equal the blocked forces.

A further interpretation can be gained through the electrical analogy. Figure 4(a) shows the equivalent electrical circuit for a source of free velocity v_{sf} and internal impedance Y_s attached to its mirror. The force and velocity at the interface (analogous to current in, and

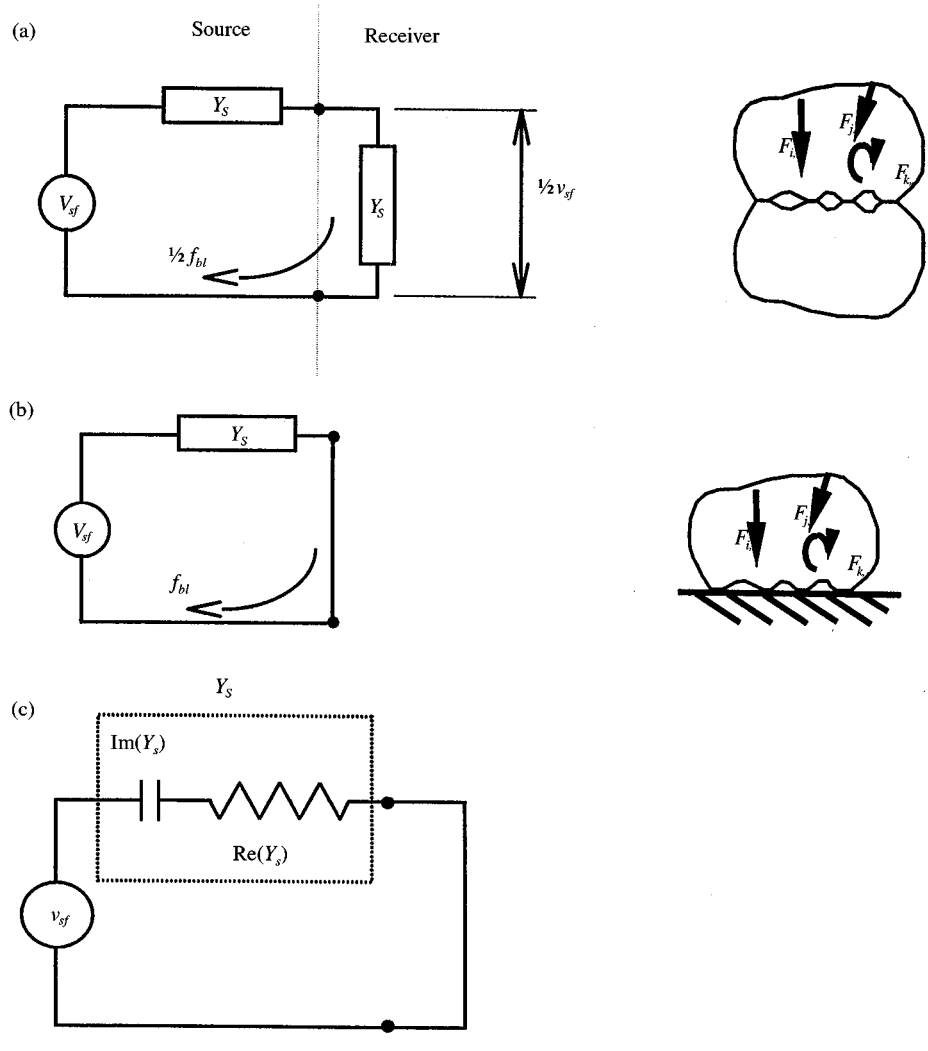

Figure 4. Equivalent electrical circuit for (a) source on mirror receiver; (b) blocked source; (c) blocked stiffness-like source.

voltage across the load) are then seen to be identically half the blocked force and free velocity respectively. The power in the load impedance is then the mirror power, that is one-quarter of the product of free velocity and blocked force, consistent with equation (8). In Figure 4(b), the source is short circuited, in which case the force and velocity are respectively f_{bl} and v_{sf}. In this case, the power is the product of free velocity and blocked force, that is the characteristic power. Thus, the CP is the power in the internal impedance of a short circuited, i.e., blocked source.

From this, one can derive a physical interpretation of the CP for a stiffness-like source with damping such as a machine flange. The electrical analogy is a source with a capacitive internal impedance in series with a resistor as shown in Figure 4(c). The time-averaged power in the capacitor is twice the radian frequency times the electrical energy stored per radian cycle. By analogy, the CP is 2ω times the time-averaged strain energy in the blocked source. The imaginary part is the power required to elastically deform the operating source

against its blocked terminals, and the real part is the power permanently dissipated in the repeated deformation. It is shown in Appendix A, by a more rigorous analysis, that the CP for a mass-like source has a similar relationship to its kinetic energy.

2.3. MAXIMUM AVAILABLE POWER FOR MULTIPLE POINT AND COMPONENT CASE

The MAP can also be extended from the single point case. The maximum power is delivered when the source and receiver are complex conjugate. By substituting $\bar{\mathbf{Y}}_R = \bar{\mathbf{Y}}_S^*$ into equation (7) one obtains

$$\bar{S}_a = \tfrac{1}{4}\,\bar{\mathbf{v}}_{sf}^{\mathrm{H}}[\mathrm{Re}(\bar{\mathbf{Y}}_S)]^{-\mathrm{H}}\bar{\mathbf{Y}}_S^{\mathrm{H}}[\mathrm{Re}(\bar{\mathbf{Y}}_S)]^{-1}\bar{\mathbf{v}}_{sf}. \tag{12}$$

As with the single point case, the expression for the real part is simpler, i.e.,

$$\mathrm{Re}(\bar{S}_a) = \tfrac{1}{4}\bar{\mathbf{v}}_{sf}^{\mathrm{H}}[\mathrm{Re}(\bar{\mathbf{Y}}_S)]^{-1}\bar{\mathbf{v}}_{sf}. \tag{13}$$

This is the maximum power that can be drawn from the source for any choice of receiver structure. Again, it is an independent property, characteristic of the source's ability to deliver power and is a single value.

2.4. DISCUSSION OF MIRROR POWER, CP AND MAP

It is noteworthy that the above three quantities independently characterize the source in terms of power. It is usually considered necessary to achieve a free or blocked mounting condition to maintain independence of the source, and in neither of these conditions is there transmission of power into a receiver. In the case of a mirror and a conjugate receiver, power transmission to the receiver does occur, but independence is maintained because the receiver is defined purely in terms of the source. It should, however, be recognized that the mirror and conjugate receivers are theoretical concepts permitting independent characterization of the source and are not necessarily achievable in practice. Since the mirror power and CP are related by a constant factor of four for both the single point and the general case, there is no need to retain both definitions. Thus, the mirror power will now be dropped and the following discussion provides a comparison between CP and MAP.

The MAP is initially a more attractive characterization because it provides the upper bound to the emission of the installed source. However, there are two disadvantages arising from its dependence on the real part of the mobility (equations (12) and (13)). Firstly, for mass- and stiffness-like sources, the mobility is purely imaginary and the maximum available power is therefore infinite. This does not violate the principle of conservation of energy, since when connected to a receiver the power delivered remains finite. Nevertheless, in such situations, which cover practically important classes of sources, the CP (which is finite and related to the kinetic energy of a mass-like source, and the strain energy in a blocked stiffness-like source) provides more useful information about the overall source strength. Secondly, it will be seen later that the MAP is sensitive to measurement errors, particularly the real part (equation (13)) which requires inversion of the real part of the mobility matrix, itself sensitive to measurement errors. The CP is much less sensitive to such errors. Thus, the following development focuses on CP rather than MAP.

It is instructive to compare CP and MAP with the much better known concept of airborne sound power, W. Airborne sound power is the power delivered by the operating source into a standardized receiving medium, generally air under freefield conditions. CP

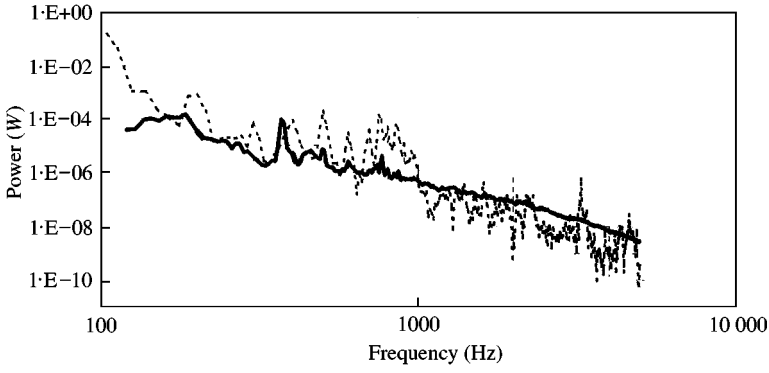

Figure 5. Characteristic power (------) of a fan compared with its airborne sound power (▬▬).

and MAP also represent power delivered to a specific receiving medium, but one that is defined in terms of source properties only, i.e., respectively, a mirror and a complex conjugate structure.

3. EXAMPLES OF CHARACTERISTIC POWER

3.1. CENTRIFUGAL FAN 1

Figure 5 illustrates the magnitude of the CP for a centrifugal fan. It was obtained using equation (9) from the measured free velocity and mobility data. Free velocity was measured at each of the four contact points in three degrees of freedom corresponding to bending vibration, i.e., normal to the surface and rotation about the two perpendicular in-plane axes. A reference channel was used to establish phase, so that $\mathbf{v}_{sf}$ was a complex 12×1 vector. The mobility was measured for the same points, and for the same degrees of freedom, giving a 12×12 matrix. Moment mobilities were measured using a moment actuator [12].

The airborne sound power is also shown in Figure 5 for comparison. It is seen that for this particular fan and operating duty, the airborne power and the characteristic power are comparable in magnitude over much of the frequency range. It should be remembered that the structure-borne emission when installed may differ from the characteristic power. Nevertheless, the ability to compare airborne and structure source strength in this way is likely to be of interest to many practitioners.

3.2. CENTRIFUGAL FAN 2

In Figure 6, the real part of the CP for a second fan is shown. The measurement and calculation procedures were essentially the same as above.

These examples illustrate two practical difficulties in obtaining characteristic power in this way. Firstly, extensive, and at times difficult measurements were required to obtain a full set of mobilities and free velocities. This level of measurement would not be practical in most situations, and negates some of the potential advantages of the simple formulation. Secondly, even if a full data set can be obtained, it inevitably contains errors. The effect is illustrated in Figure 6, where the real part rather than the magnitude of the CP has been plotted. This shows that at a few frequencies the calculated real part was negative (the

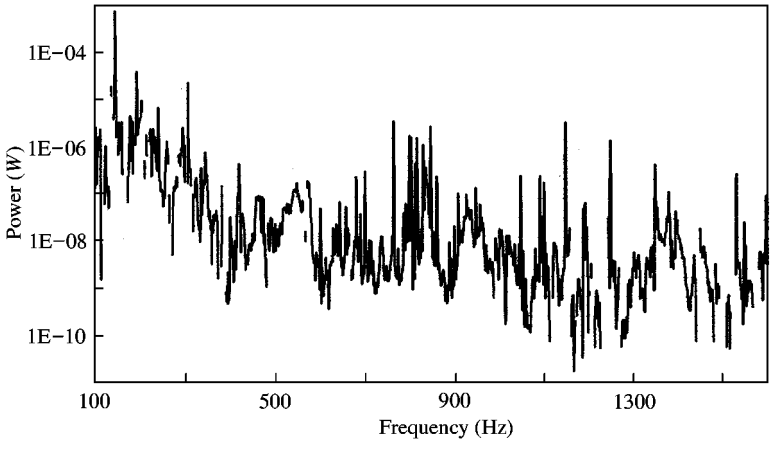

Figure 6. Real part of CP for a fan on a plate-like base.

missing sections of the curve). This is "unphysical" the anomaly being due to errors in the measured mobilities which are amplified during the matrix inversion (similar anomalies were obtained from the results of fan 1). It is unlikely that this problem can be completely avoided by more accurate measurements, since errors of the order of 1 dB are inevitable which, for matrix operations involving many elements are relatively large.

An alternative approach is to characterize the essential behaviour of the source, for example as mass-like, beam-like, plate-like, etc. [13, 14] and then to calculate mobility matrices so as to simultaneously reduce the measurement requirement and provide self-consistent data which will withstand operations like matrix inversion. The analysis presented in Appendix A for a mass-like source illustrates some of the advantages of such an approach.

4. EMISSION FROM INSTALLED SOURCES AND THE COUPLING FACTOR

It was stated in the introduction that a useful source descriptor needs to form a basis for the calculation of emission into a known receiver structure. Such possibilities are examined in this section.

4.1. EMISSION IN TERMS OF CP

By emission is meant the complex power through the interface of a source and a given receiver, as described by equations (1) and (7). Initially, consider a single point contact, for which Mondot and Petersson rewrite equation (1) as

$$\bar{Q} = \bar{S}\,\bar{C}, \tag{14}$$

where $\bar{C} = \bar{\alpha}/|1 + \bar{\alpha}|^2$ is the dimensionless "coupling function", given in terms of the mobility ratio $\bar{\alpha} = \bar{Y}_R/\bar{Y}_S$, and $\bar{S} = |\bar{v}_{sf}|^2/(\bar{Y}_S)^*$ is the source descriptor.

Here, a "coupling factor" will be defined as the constant of proportionality between the complex emission and the magnitude of the CP.

$$\bar{C}_c = \bar{Q}/|\bar{S}_c|. \tag{15}$$

This ratio was expressed as a function of $\bar{\alpha}$ and the receiver mobility phase in equation (2).

The new term "coupling factor" has been introduced as the definition is not identical to Mondot and Petersson's coupling function, the normalization being with respect to the magnitude of the CP rather than the complex source descriptor. At first sight, Mondot and Petersson's coupling function is more elegant because it depends only on the complex mobility ratio whereas the coupling factor as introduced above is also a function of receiver mobility phase. However, this advantage is lost when looking at the real part of the emission, (which is of most practical interest). Furthermore, definition 18 has the advantage that the phase of the emission is identical to that of the coupling factor. Hence, in the following sections, the normalization of the emission will be with respect to $|\bar{S}_c|$ rather than complex $\bar{S}_c$.

The coupling factor as defined in equation (15) extends directly to the multiple point and component case. In this way, the multiple point and component model has been reduced to an equivalent single point model whilst maintaining the independence of the source. $\bar{C}_c$ can also be given in terms of the source and receiver mobilities by substituting equations (15) and (9) into equation (7). It is expected that the coupling factor will follow the same basic trends as for the single point case as illustrated in Figure 2. The only additional difficulty for multiple point contact is the interpretation of the mobility ratio $\bar{\alpha}$. Some insight in this respect can be gained by recognizing that the exact form of Figure 2 is followed in the theoretical case when the receiver mobility is a scalar multiple of that of the source, i.e., when

$$[\bar{\mathbf{Y}}_R] = \bar{\alpha}[\bar{\mathbf{Y}}_S], \tag{16}$$

where $\bar{\alpha}$ is a complex constant, and $[\bar{\mathbf{Y}}_R]$ and $[\bar{\mathbf{Y}}_S]$ are the receiver and source mobility matrices. The x-co-ordinate is then simply $|\bar{\alpha}|$. The lower curve in Figure 2 is followed if the constant $\bar{\alpha}$ is real. Relationship (4) suggests a fictive receiver which is mathematically similar to the source but larger or smaller by a constant value. Unfortunately, in general an increase or decrease in physical size of the receiver structure does not scale all elements of the mobility matrix equally, and the simple relationship equation (16) is not physically realizable. Nethertheless, the concept is useful at least in a qualitative sense.

A similar coupling factor can be defined corresponding to the MAP. This is interesting because it has a maximum possible value of unity and can therefore be considered a thermodynamic efficiency factor. However, this will not be pursued in this paper.

5. EXAMPLES OF EMISSION BY INSTALLED SOURCES

5.1. FANS

The power delivered from fan 2 into three different receiver structures has been calculated; an infinite 3 mm steel plate, a frame of steel beams, and an infinite 150 mm concrete slab. Measured mobility and free velocity data was used for the source. Mobilities of the beam frame were measured using the same techniques as for the source (see above and reference [12]). Mobilities for the infinite plates were obtained analytically using the solution for point contact [15] which was differentiated to obtain moment and cross mobilities. A contact radius of 50 mm was assumed for the point moment mobilities without which the imaginary part becomes infinite. In all cases, both source and receiver structures were characterized by 12×12 mobility matrices. Power was calculated from equation (7) the CP from equation (9) and the coupling factor from equation (15).

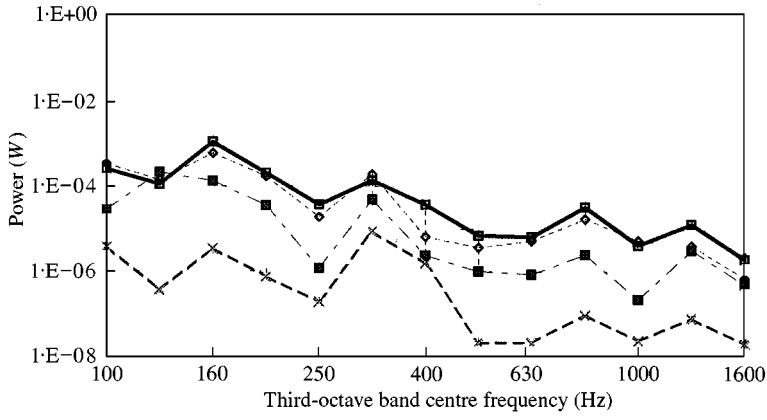

Figure 7. CP of a fan on a plate-like base, and emission to various receivers. —□—, characteristic power, $|S|$; - -◇- -, 3 mm steel plate; —■—, beam frame; – – ×, 150 mm concrete plate.

The power delivered (real part) to each receiver is shown in third-octave bands in Figure 7. Power transfer to the steel plate is seen to be most efficient, which is not surprising, given that this was the same thickness and material as the base plate of the fan and therefore well matched. The least efficient power transfer was to the concrete plate, and again this was anticipated because of the large mobility mismatch. Power transfer to the beam frame was less efficient than to the steel plate, even though the point mobilities were of similar magnitude to those of the fan over most of the frequency range. This could be because the moment, cross and transfer mobilities would match less well for a plate/beam interface than for a plate/plate interface, which is in accord with the speculation made above that power transfer is most efficient in receivers similar to the source. Note that in no case does the delivered power significantly exceed the CP, even for well-matched receivers.

5.2. BEAM SOURCE ON PLATE RECEIVERS

In the previous example, and others involving real sources, the mobility data inevitably contains errors which do not help to clarify trends in behaviour. Hence, further examples have been treated using analytical models. The second example consists of an analytical model of a pump, connected via pipework to a large plate.

The pipe was modelled as a beam with added mass to represent the enclosed water, and the internal operating forces of the pump were represented as a frequency invariant force applied to the pipe non-symmetrically between the contact points as shown in Figure 8. Even for this idealized model, the transfer at the interface is relatively complicated, with a force and moment excitation at each point giving a 4×4 mobility matrix. The emission from this idealized pump was calculated when connected to infinite plates with eight different thicknesses and material properties.

In Figure 9, the CP for this idealized pump is shown. The spectrum contains strong peaks at frequencies where the contact points are separated by 3/4, 5/4, 7/4, … wavelengths due to simultaneous constructive interference in both rotational and translational response. Even though the pipe response, being that of an infinite structure, is a relatively smooth function of frequency, the peaks in CP are relatively sharp and pronounced. If the position of the

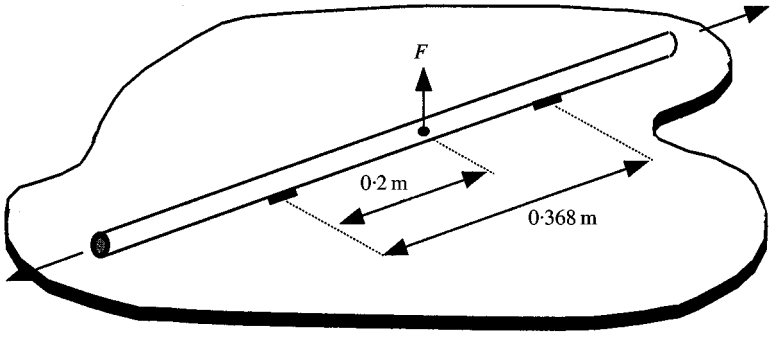

Figure 8. Idealized pump on infinite plate receiver.

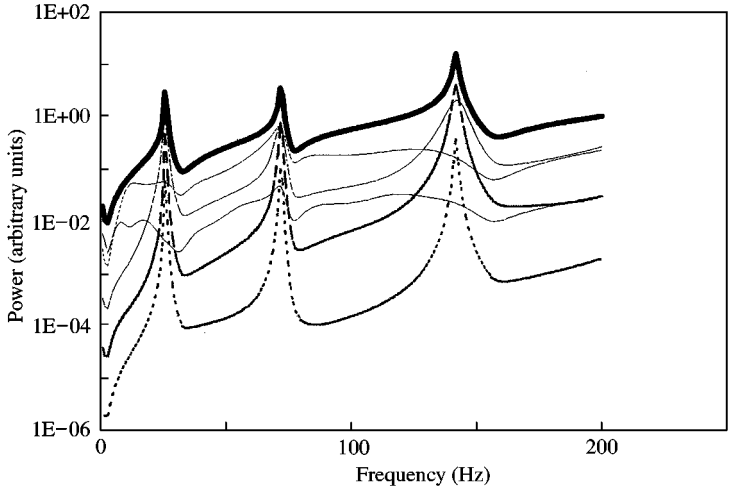

Figure 9. CP of an idealized pump, and emission into various infinite plate receivers defined in Table 1. ——, $|S_c|$, Base plate materials; - - -, A; – – –, C; — — —, D; ------, F; -·-·-, H.

exciting force is modified the relative magnitude of these peaks varies, but their frequencies remain the same. On the same plot the emission (real part) into various plate receivers is shown. As in Figure 7, the emission is generally less than the CP depending on how well matched the source are receiver are.

Figure 10 illustrates the same data as in Figure 9, but rather than plotting against frequency, the x-co-ordinate is taken as the ratio of the ordinary point mobilities of the infinite beam and plate $|Y_R|/|Y_S|$. Additionally, the real part of the emission is normalized by the magnitude of the CP, so that the plotted values are the real part of the coupling factor. The straight lines are the asymptotes corresponding to the free and blocked sources, respectively, as seen from the single point case illustrated in Figure 2. They have slopes of ± 1 and intersect when the dimesionless power is of unit magnitude. The dimensionless power is seen to follow the skeleton formed by these asymptotic lines.

A second point of interest is that the dimensionless power does not exceed unity. This is in agreement with the findings of the previous section, and provides more evidence that the CP may effectively be the "available power" in many practical situations.

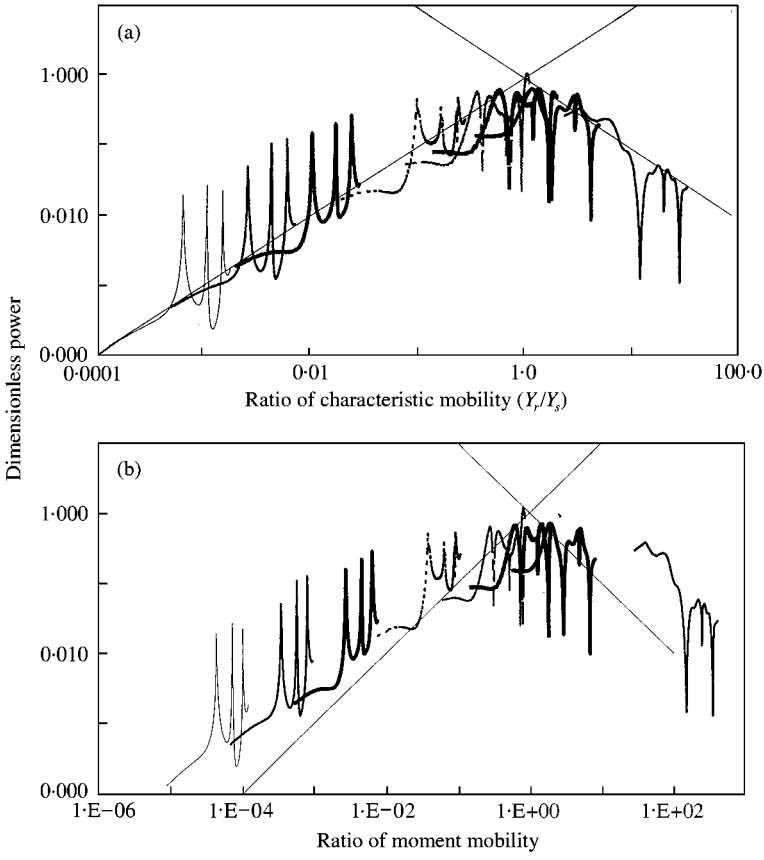

Figure 10. Dimensionless emission from an idealized pump into various infinite plate receivers (defined in Table 1) as a function of (a) ordinary point mobility ratio, (b) moment mobility ratio. Base plate materials: ——, F; ——, E; ▬▬, D; ------, C; — · — · —, B; — – —, G; ▬▬, A; ——, H.

The peaks in the dimensionless power correspond to those in the CP. It is seen that peaks are pronounced, and above the skeleton lines by more than a decade for low mobility receivers ($|\bar{\alpha}| \ll 1$), are less pronounced around $|\bar{\alpha}| = 1$, and fall below the skeleton lines for $|\bar{\alpha}| \gg 1$. This is not a general result, but is due to coupling between the contact points taking place within the beam source. It is expected that coupling within the beam would be stronger than in the plate because of circular spreading losses in the plate. For thick and heavy plate receivers, the source dominates the coupling and the peaks show through (i.e., the term $Y_S + Y_R$ in equation (7) is dominated by Y_S). For light and thin plate receivers, the plate mobility dominates the coupling, and interaction within the beam source is less evident.

This choice of ordinary point mobility ratio for the x-axis of Figure 10(a) is to an extent arbitrary, as moment mobilities or some other single measure of the mobility matrices could equally have been taken. Figure 10(b) illustrates the same data, replotted in terms of moment mobility ratio. The dimensionless power follows the trend lines less faithfully than in Figure 10(a). This suggests that for this case, moments have less influence on the emission than normal forces, but again this is not necessarily a general result.

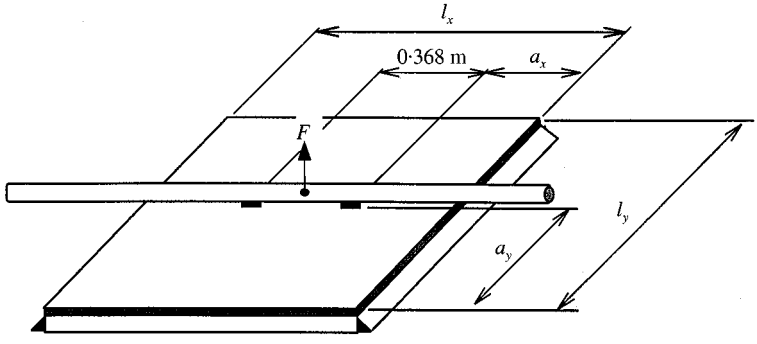

Figure 11. Idealized pump on SSSS plate receiver.

TABLE 1

Properties of receiver plates for Figures 8–12

Plate	Material	Thickness (mm)	Density (kg/m^3)	Wave speed (m/s)	l_x (m)	l_y (m)	a_x (m)	a_y (m)
A	Plasterboard	9	780	4150	0·6	1·0	0·1	0·4
B	Plasterboard	19	780	4150	0·6	1·0	0·1	0·4
C	Plasterboard	38	780	4150	0·6	1·0	0·1	0·4
D	Concrete	75	2600	3100	3·2	2·6	1·5	1·0
E	Concrete	150	2600	3100	3·2	2·6	1·5	1·0
F	Concrete	300	2600	3100	3·2	2·6	1·5	1·0
G	Plywood	19	600	3000	0·6	1·0	0·1	0·4
H	Steel	1	7800	5000	0·6	1·0	0·1	0·4

5.3. BEAM SOURCE ON FINITE PLATE RECEIVERS

In the previous example, it was found that the emission never exceeded $|\bar{S}_c|$, even for source and receiver mobilities of equal magnitude. The reason could be that their phase is fixed (0 and $\pi/4$, respectively, for an infinite plate and an infinite beam), so source and receiver can never be complex conjugate to one another (this being the condition under which the maximum available power is delivered). Finite structures are more likely to be complex conjugate, because the phase of their mobilities varies rapidly, and hence, the conditions where emission exceeds $|\bar{S}_c|$ are more likely to arise.

In order to test this, the above source was assumed attached to finite, rectangular plate receiver, simply supported at all edges, in place of the infinite plate. Mobilities for the plate were obtained from the well-known series solution [15], with moment mobilities obtained by differentiation. Properties and dimensions of the plates are shown in Figure 11 and Table 1. A loss factor of 5% was assumed in the plate.

Results are shown in Figure 12 plotted versus the ratio of characteristic mobilities (infinite beam and plate mobilities). The dimensionless emission follows the trend lines in a way similar to Figure 10, but with resonances superimposed. $|\bar{S}_c|$ is exceeded at some points when mobilities are matched in magnitude. The same trends were observed when plotting against the actual ratios of point force mobility at the two contact points, but the resulting plot was "messy" and is not shown.

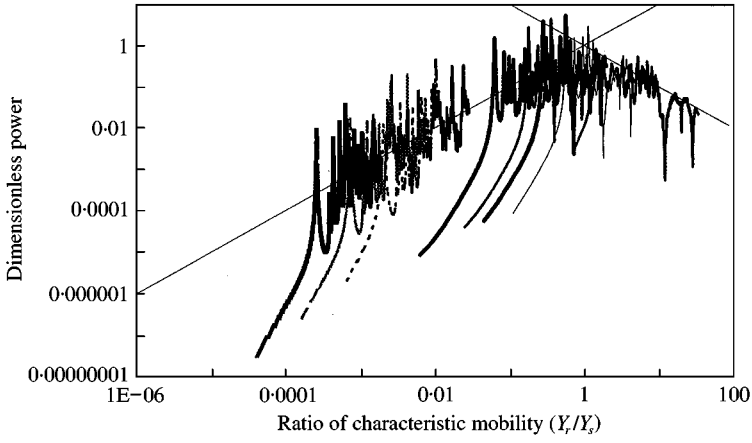

Figure 12. Dimensionless emission from an idealized pump to various SSSS plate receivers (defined in Table 1) versus ratio of characteristic mobility. Base plate materials: ——, A; ——, B; ▬, C; - - - - -, D; — — —, E; — · —, F; ▬, G.

6. CONCLUDING REMARKS

Three possible descriptors for structure-borne sound sources have been presented, the characteristic power (CP), mirror power and maximum available power (MAP). All three are independent properties of the source, and characterize its ability to transmit structure-borne sound power accounting for all mechanisms such as forces and moments. All are single, frequency-dependent quantities which will facilitate potentially useful comparisons between sources, and with other descriptors such as airborne sound power and fluid-borne power for pumps.

The MAP initially appears the more elegant because it provides a rigorous upper bound to the emission. However, the CP is more robust and is thought more likely to answer the requirements of practising engineers. It is relatively easily visualized as 4 times the emission into a mirror receiver. Furthermore, whilst MAP is the theoretical maximum emission from a given source, the CP provided an effective upper bound to emission in some of the case studies treated. Further theoretical work is needed to establish for which combinations of practical structures the emission will exceed CP.

Difficulties of matrix inversion mean that obtaining the CP purely by measurement is likely to be problematic. However, these practical difficulties are inherent in any attempt to characterize structure-borne sound sources, and do not devalue the theoretical importance of the CP. A way forward is to develop simplified measurement, and combined measurement and calculation methods, which must be based on an understanding of the structural dynamic behaviour of the source.

Probably, the most important property of the CP is that it provides an equivalent single-point model for multiple-point connected sources and receivers. As a result, it is possible to superimpose the coupling factor for realistic source–receiver combinations on the skeleton plot for single point contact. The emission, not surprisingly, follows the same trends as the single point case, but with some variation about the trends due to coupling between degrees of freedom. This provides a basis for simple estimates of the coupling factor and hence emission, based solely on the ratio of source to receiver mobility. At the current state of development the band of accuracy for such estimates is not known, and further

work is proposed to establish upper and lower bounds for particular structural types. However, such estimates will be within the scope of many practising engineers who currently lack any methodology for quantifying the importance of structure-borne sound sources.

ACKNOWLEDGMENTS

This work was funded by the Science and Engineering Research Council whose support is gratefully acknowledged. The assistance of Dr N Backhouse, University of Liverpool is also gratefully acknowledged.

REFERENCES

1. T. TEN WOLDE and G. R. GADEFELT 1987 *Noise Control Engineering Journal* **28**, 5–14. Development of standard measurement methods for structure-borne sound emission.
2. INTERNATIONAL STANDARDS ORGANISATION 1996 *ISO* 9611. Acoustics—characterisation of sources of structure-borne sound with respect to sound radiation from connected structures—measurement of velocity at the contact points of machinery when resiliently mounted.
3. J. LU, B. LOUVIGNE, J. C. PASCAL and J. TOURRET 1990 *Proceedings Inter-Noise*' 90, 217–220. The perforated reception plate; a practical method for the characterisation of structure-borne noise emitted by small equipment.
4. N. QI and B. M. GIBBS 1999 *Proceedings Inter-Noise*'99, 757–762. Fort Lauderdale, small circulation pumps as structure-borne noise sources.
5. S. STEFFENATO 1999 *Proceedings of the Sixth International Congress on Sound and Vibration*, Lyngby, 2223. Correlation between refrigerator noise and compressor vibrations. Development of a new measurement method for compressor vibrations.
6. J. W. VERHEIJ 1997 *International Journal of Acoustics and Vibration* **2**, 11–20. Inverse and reciprocal methods for machinery noise source characterisation and sound path quantification.
7. M. OHLRICH 1998 *Proceedings Euronoise*'98, *Munich*, 383–388. *A simple structural power method for determining the vibratory strength of machinery sources.*
8. *R. J. PINNINGTON and D. C. PEARCE* 1990 *Journal of Sound and Vibration* **142**, 461–479. Multipole expansion of the vibration transmission between a source and a receiver.
9. J. M. MONDOT and B. A. T. PETERSSON 1987 *Journal of Sound and Vibration* **114**, 507–518. Characterization of structure-borne sound sources: the source descriptor and the coupling function.
10. A. T. MOORHOUSE, J. M. MONDOT and B. M. GIBBS 1997 *Proceedings of the Fifth International Congress on Sound and Vibration*, Adelaide, 2449. Source descriptors for structure-borne sound sources.
11. B. A. T. PETERSSON and J. PLUNT 1982 *Journal of Sound and Vibration* **82**, 517–540. On effective mobilities in the prediction of structure-borne sound transmission between a source and a receiver structure. Part 1: theoretical background and basic experimental studies', and Part 2: procedures for the estimation of mobilities.
12. J. M. MONDOT and A. T. MOORHOUSE 1996 *Proceedings Inter-Noise*'96, *Liverpool*, Book 3, 1439–1446. The characterisation of structure-borne sound sources.
13. R. A. FULFORD and B. M. GIBBS 1999 *Journal of Sound and Vibration* **220**, 203–224. Structure-borne sound power and source characterisation in multi-point-connected systems. Part 2: about mobility functions and free velocities.
14. B. M. GIBBS and A. T. MOORHOUSE 1999 *International Journal of Acoustics and Vibration* **4**. Case studies of machine bases as structure-borne sound sources in buildings.
15. L. CREMER, M. HECKL and E. E. UNGAR 1973 *Structureborne Sound*. Berlin: Springer-Verlag.
16. B. A. T. PETERSSON and B. M. GIBBS 1993 *Journal of Sound and Vibration* **168**, 157–176. Use of the source descriptor concept in studies of multi-point and multi-directional vibrational sources.
17. A. T. MOORHOUSE and B. M. GIBBS 1998 *Acustica* united with *Acta Acustica* **84**, 843–853. Simplified characterisation of multiple point excited structures using mobility matrix eigenvalues and eigenvectors.

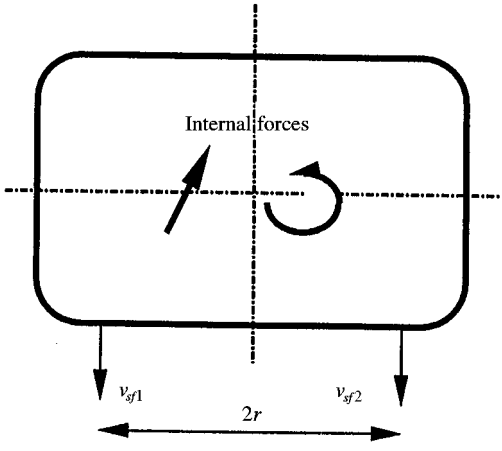

A1. Idealized rigid mass source.

APPENDIX A: CP FOR A MASS-LIKE SOURCE

Structure-borne sound sources can be idealized as rigid masses at frequencies where the governing wavelength is significantly longer than the dimensions of the structure. For compact sources, this frequency region can extend over a large part of the range of interest. Figure A1 shows an idealized, two-dimensional mass source in which the unknown internal operating forces of the machine are represented by any physically realizable combination of applied forces. The source is represented by its mass, M and radius of gyration, p. The characteristic power is given by the quadratic form

$$\bar{S}_c = \mathrm{j}\omega \mathbf{M}\{\bar{\mathbf{v}}_{s1}\,\bar{\mathbf{v}}_{s2}\}^* \begin{bmatrix} 1 + r^2/p^2 & 1 - r^2/p^2 \\ 1 - r^2/p^2 & 1 + r^2/p^2 \end{bmatrix}^{*-1} \begin{Bmatrix} \mathbf{v}_{s1} \\ \mathbf{v}_{s2} \end{Bmatrix}. \tag{A1}$$

This can be solved by expanding the free velocity vector in terms of the eigenvectors of the mobility matrix, thus decomposing the problem into a "bouncing" mode and a "rotating" mode (see references [8, 16, 17]). The characteristic power is then the sum of the contributions of these two modes, namely bouncing mode $\bar{S}_c = |\tilde{v}_{sf}|^2 M\mathrm{j}\omega$ and rotating mode $\bar{S}_c = |\tilde{v}_{sf}|^2 (p^2/r^2) M\mathrm{j}\omega$, where $|\tilde{v}_{sf}|$ is the free velocity magnitude averaged over the two points. In both the case of the bouncing and the rotation modes, the characteristic power is simply $2\mathrm{j}\omega$ times the kinetic energy. This result extends to mass-like sources with any number of contact points and degrees of freedom. Thus, in general for a mass

$$\bar{S}_c = 2\mathrm{j}\omega \times \text{kinetic energy}.$$

It can be recalled that a derivation via the electrical analogy in the introduction showed there to be a parallel relationship to strain energy for a stiffness-like source. This result is of practical significance because the kinetic energy can be obtained with a maximum of six free velocity measurements which are not restricted to the contact points. Also, the mass and moments of inertia can be accurately obtained by calculation or static measurements.

APPENDIX B: EXTENSION OF THE CONCEPT OF MAP TO THE MULTIPLE POINT CASE

A formal mathematical proof of the extension of equation (3) to multiple points is long, and will not be given here. However, the validity can be illustrated relatively easily for the

special case of geometrically symmetric structures. In this case, equation (3) can be written as a weighted sum of eigenvalues [17]:

$$\bar{Q} = \bar{\mathbf{v}}_{sf}^{\mathrm{H}}[(\bar{\mathbf{Y}}_S + \bar{\mathbf{Y}}_R)^{-\mathrm{H}}\bar{\mathbf{Y}}_R(\bar{\mathbf{Y}}_S + \bar{\mathbf{Y}}_R)^{-1}]\bar{\mathbf{v}}_{sf} = \sum_{i=1}^{n} |\bar{a}|^2 \bar{\lambda}_i, \tag{B1}$$

where $\bar{\lambda}_i$ are the eigenvalues of the square, complex symmetric matrix in square brackets. This can be written in terms of the eigenvalues of the constituent matrices, since in the symmetric case, $\bar{\mathbf{Y}}_R$ and $\bar{\mathbf{Y}}_S$ share common eigenvectors

$$\bar{Q} = \sum_{i=1}^{n} |\bar{a}|^2 \frac{\bar{\lambda}_{R,i}}{|\bar{\lambda}_{R,i} + \bar{\lambda}_{S,i}|^2}, \tag{B2}$$

where $\lambda_{R,i}$, $\lambda_{S,i}$ are the complex eigenvalues of $\bar{\mathbf{Y}}_R$ and $\bar{\mathbf{Y}}_S$ respectively. Each term in the above sum is of the form of the (1×1) case given in equation (1), and its real part and magnitude is maximized when $\lambda_{R,i} = \lambda_{S,i}^*$. The multiple point case can therefore be considered to be made up of a sum of equivalent single point cases, and the extension from single to multiple point interfaces is valid.